

Gene Therapy Rescues Retinal Degeneration in Receptor Expression-Enhancing Protein 6 Mutant Mice

Smriti Agrawal Zaneveld,^{1,2} Aiden Eblimit,^{1,2,†} Qingnan Liang,^{1,3} Renae Bertrand,^{1,3} Nathaniel Wu,^{1,2} Hehe Liu,^{1,2} Quynh Nguyen,³ Jacques Zaneveld,^{1,2} Keqing Wang,^{1,2} Yumei Li,^{1,2} and Rui Chen^{1,2,*}

¹Human Genome Sequencing Center, ²Department of Molecular and Human Genetics, and ³Department of Biochemistry, Baylor College of Medicine, Houston, TX.
[†]Current address: Department of Biomedical Engineering, University of Houston, Houston TX.

Hereditary retinal dystrophy is clinically defined as a broad group of chronic and progressive disorders that affect visual function by causing photoreceptor degeneration. Previously, we identified mutations in the gene encoding receptor expression-enhancing protein 6 (REEP6), in individuals with autosomal recessive retinitis pigmentosa (RP), the most common form of inherited retinal dystrophy. One individual was molecularly diagnosed with biallelic *REEP6* mutations, a missense mutation over a frameshift mutation. In this study, we generated *Reep6* compound heterozygous mice, *Reep6*^{L135P/-}, which mimic the patient genotype and recapitulate the early-onset retinal degeneration phenotypes observed in the individual with RP. To determine the feasibility of rescuing the *Reep6* mutant phenotype via gene replacement therapy, we delivered *Reep6.1*, the mouse retina-specific isoform of *REEP6*, to photoreceptors of *Reep6* mutant mice on postnatal day 20. Evaluation of the therapeutic effects 2 months posttreatment showed improvements in the photoresponse as well as preservation of photoreceptor cells. Importantly, guanylyl cyclase 1 (GC1) expression was also restored to the outer segment after treatment. Furthermore, rAAV8-*Reep6.1* single treatment in *Reep6* mutant mice 1 year postinjection showed significant improvements in retinal function and morphology, suggesting that the treatment is effective even after a prolonged period. Findings from this study show that gene replacement therapy in the retina with rAAV overexpressing *Reep6* is effective, preserving photoreceptor function in *Reep6* mutant mice. These findings provide evidence that rAAV8-based gene therapy can prolong survival of photoreceptors *in vivo* and can be potentially used as a therapeutic modality for treatment of patients with RP.

Keywords: blindness, gene therapy, human disease, inherited retinal dystrophy, REEP6, retinitis pigmentosa

INTRODUCTION

RETINITIS PIGMENTOSA (RP) is a heterogeneous genetic disease of the eye, which is characterized by retinal degeneration that results in irreversible loss of light-sensing neurons in the retina, called photoreceptors. In RP, the rod photoreceptors, which play essential roles in providing dark and peripheral vision, are affected first, followed by progressive degeneration of the cones, which provide color and fine-detailed vision.^{1,2} Ultimately, the progressive nature of the disease leads to loss of visual acuity and can lead to complete blindness.¹⁻⁵ Over the past decades, pathogenic variants in more than 85 genes have been identified that can be

transmitted through different modes of inheritance, and at least 60 genes have been identified to be associated with autosomal recessive RP (arRP).^{6,7} However, mutations in these genes can explain the genetic basis of approximately 60% of RP cases, leaving 40% of the patients without a molecular diagnosis.⁴ Thus, in efforts to identify pathogenic variants underlying retinal dystrophy, we performed a large-scale screen, using whole-genome and whole-exome sequencing, which led to the identification of mutations in a gene encoding receptor expression-enhancing protein 6 (*REEP6*). Specifically, we identified individuals with *REEP6* variants in five unrelated families from diverse

*Correspondence: Dr. Rui Chen, Department of Molecular and Human Genetics, Baylor College of Medicine, Houston, TX 77030. E-mail: ruichen@bcm.edu

ethnicities that were clinically diagnosed with non-syndromic RP.⁴ Although the nature of the mutations identified varied, the affected individuals were diagnosed with nyctalopia, visual field constriction and peripheral retinal atrophy, severely impaired or diminished responses to light as measured by electroretinograms,⁸ marked reduction in the thickness of the overall retina and photoreceptor outer nuclear layer, and characteristic deposition of bone spicule-like pigments in their fundus.⁴ Interestingly, studies have identified several additional RP families with *REEP6* variants that also lead to retinal degeneration,^{9,10} further exemplifying the significance of *REEP6* in photoreceptor function and survival.

REEP6 belongs to the *REEP* family of proteins, which have previously been implicated in enhancing expression of cell surface receptors and in endoplasmic reticulum (ER) membrane shaping.^{11–16} *REEPs* are homologous to the yeast *Yop1/Yip* proteins, which have been shown to regulate intracellular trafficking and targeting of vesicle cargos, particularly G protein-coupled receptors ($\alpha 2A$ and $\alpha 2C$ adrenergic receptors), to the plasma membrane via interaction at the carboxyl termini.¹⁵ In addition, they function as membrane-shaping adapter proteins and are described as ER morphogens.¹³ When *Reep6* was first cloned, it was referred to as deleted in polyposis 1-like 1 (*Dp111*) as it was highly homologous to a mouse homolog (*Dp1*) of the human gene *TB2/DP1*, and *in situ* hybridization showed that *Dp111* mRNA was abundantly expressed in the retinal ganglion cells.¹⁷ Furthermore, gene expression profiling of mice deficient in *Nrl*, which encodes the Maf-family leucine zipper transcription factor NRL, revealed that *Reep6* is directly regulated by NRL, which is specifically expressed in rod photoreceptors in the retina.¹⁸ We and other have shown that *REEP6* is predominantly expressed in rod photoreceptors, specifically in the endoplasmic reticulum, and is absent from cone photoreceptors.^{3,4,9} Mice carrying mutations in *Reep6* show a phenotype similar to that of human patients. Specifically, *Reep6*^{L135P} knock-in (KI) mice, which harbor a missense variant seen in a patient, exhibit adult-onset retinal dysfunction and photoreceptor degeneration, demonstrating that the p.Leu135Pro missense variant is indeed pathogenic. *Reep6* null mice present with a more severe, early-onset phenotype of photoreceptor dysfunction that precedes photoreceptor degeneration.³ Therefore, *Reep6* mutant mice can serve as a good model to study human disease.

One of the interesting observations in *Reep6* mutant mice is that the reduction in electroretinogram (ERG) response occurs before obvious photoreceptor

degeneration. One explanation for this phenotype is that it is likely due to altered trafficking and/or stability of specific proteins involved in the phototransduction pathway, including guanylyl cyclase, phosphodiesterase 6 (PDE6), transducin- α , and G protein subunit α transducin 1 (GNAT1), in *Reep6* mutant mice. Defects in delivery of proteins to their specific subcellular compartments in the photoreceptors can lead to severely compromised regulation of the phototransduction cascade, evident in *Reep6*-deficient mice as well as several other retinal disease models.^{19–24} Furthermore, *Reep6* knockout (KO) mice exhibited ER stress and induction of the unfolded protein response pathway, as well as abnormal mitochondrial proliferation, likely resulting from protein transportation defects in photoreceptors, leading to a progressive loss of vision.

Given that loss of *REEP6* leads to severe perturbation of retinal function in individuals with RP and that the associated disease pathogenesis is progressive, it provides us an opportunity to devise new treatment strategies for *REEP6*-associated RP. Adeno-associated virus (rAAV)-based gene therapies have been shown to be successful in rescuing disease phenotypes in several animal models of retinal degeneration^{25–38} as well as in patients.^{7,39–42} Indeed, most recently, RPE65 gene therapy became the first directly administered treatment approved by the U.S. Food and Drug Administration for patients with Leber congenital amaurosis 2 (LCA2; OMIM entry MIM204100) and retinitis pigmentosa 20 (RP20) (MIM#613794). rAAV vector plasmids have been studied extensively for delivery of functional genes in various cell types in the retina. Specifically, the rAAV serotype 8 (rAAV8) vector plasmid can provide high transduction efficiency and rapid expression of transgenes in photoreceptor cells under the control of the human rhodopsin kinase (hGRK1) promoter.^{31,32,36}

In this study, we generated and characterized compound heterozygous mice harboring a combination of the missense p.Leu135Pro allele and a loss-of-function allele, recapitulating the *REEP6* variants identified in an individual with simplex RP.^{3,4} *Reep6*^{L135P/-} compound heterozygous mice exhibit photoreceptor degeneration starting at 1 month of age, which worsens in severity over time. Using the *Reep6*^{L135P/-} mice as an animal model for gene therapy, we evaluated whether delivery of murine *Reep6.1*, the retina-specific isoform of *REEP6*, to photoreceptors of postnatal *Reep6* mutant mice could preserve photoreceptor function and survival. We used rAAV8 to deliver *Reep6.1* in the retina of postnatal day 20 (P20) *Reep6*^{L135P/-} mice and show for the first time that rAAV8-*Reep6.1*

gene therapy can rescue REEP6-associated retinal degeneration in mice over a course of more than 1 year. Collectively, these findings unravel the successful targeting and therapeutic effects of rAAV8-*Reep6.1*-mediated gene therapy in mice and lay a foundation for the potential of gene therapy treatments in patients with *REEP6*-associated RP.

MATERIALS AND METHODS

Production of rAAV8-*Reep6.1* viral vector

Full-length *Reep6.1* cDNA was tagged with a 3×FLAG epitope tag to the N terminus of *Reep6.1* (GENEWIZ). The 3×FLAG-tagged mouse *Reep6.1* cDNA was digested with *NotI* and amplified by PCR, and the sequence was verified. rAAV8 vector plasmid containing the G protein-coupled receptor kinase 1 (GRK1) promoter was used to generate the pTR-Grk1-3xFlag-*mReep6.1* plasmid. rAAV8 was used to package Grk1-3xFlag-*mReep6.1* to achieve robust transduction efficiency and expression in retinal photoreceptors (Gene Vector Core, Baylor College of Medicine). The resulting viral titer for rAAV8-hGrk1-3xFlag-*mReep6.1* was 7.1×10^{13} genome copies (GC)/mL. rAAV8-hGrk1(Y733F)-GFP viral vector (2.31×10^{13} GC/mL) was used as a control for subretinal injections.

Generation of *Reep6* compound heterozygous mice

Previously, *Reep6* L135P KI and *Reep6* KO mice were generated by CRISPR (clustered regularly interspaced short palindromic repeats)/*Cas9* gene editing.^{3,4} In this study, *Reep6*^{L135P/L135P} homozygous male mice were bred with *Reep6*^{+/-} heterozygous female mice to generate *Reep6*^{L135P/-} compound heterozygous mutant mice. Genotyping was performed by a genomic PCR assay as described previously,^{3,4} followed by Sanger sequencing. Genotyping analysis for *Reep6* control and mutant mice is shown in Supplementary Fig. S1. All *Reep6*^{L135P/-} compound heterozygous mutant mice were grossly normal and viable.

All mice in this study were maintained under 12-h light and 12-h dark cycle conditions. All animal experiments were conducted in agreement with the Association for Research in Vision and Ophthalmology (ARVO) statement for the use of animals in ophthalmic and vision research, and protocols were approved by the Institutional Animal Care and Use Committee (IACUC) at Baylor College of Medicine.

Subretinal injections

P20 mice were anesthetized with a combination drug consisting of ketamine (22 mg/kg), xylazine

(4.4 mg/kg), and acepromazine (0.37 mg/kg), which was injected intraperitoneally. Subretinal injections were performed as described previously.³⁶ A shallow incision was made through the sclera with a beveled 30-gauge needle. After this step, a 35-gauge blunt needle was presented inside the vitreous cavity and pushed forward until the tip of the needle had moved past the retina. Viral solution was injected into the subretinal space, using an Ultra-Micro-Pump II and Micron-4 Controller (World Precision Instruments). Mice were treated once in the right eye, using 1 μ l of rAAV8-hGRK1-3xFlag-*mReep6.1* (7.1×10^{13} GC/mL), and coinjected with rAAV8-hGRK1(Y733F)-GFP (1.0×10^{12} GC/mL) for examining transduction efficiency posttreatment, whereas the contralateral left eye was uninjected, serving as an internal control. Altogether, 20 *Reep6*^{L135P/-} mutant mice were injected for assessment 2 months posttreatment and 1 year posttreatment. In addition, eight age-matched *Reep6*^{L135P+} control mice in total were injected in the right eye to assess toxicity. No decline in visual function or morphology was observed in the right eye of control mice compared with the left untreated eye (data not shown).

Electroretinography

Before ERG, the fundus of all mice injected was evaluated for damage resulting from injections, including severe retinal detachment, atrophy, scarring using the Micron-IV retinal imaging system (Phoenix Research Laboratories). Mice were dark-adapted overnight (at least 12 h) before ERG experimentation. ERGs were performed as previously described.^{3,4,36} The anesthesia cocktail (described in the previous section) was delivered by intraperitoneal injection into the mice. Pupils were dilated under dim red light with tropicamide (1%) and phenylephrine (2.5%) eye drops, and proparacaine (1%) was used to anesthetize the cornea. Goniosoft (hypromellose, 2.5%) was applied to the cornea to avoid dehydration and facilitate contact before placing ERG electrodes on each eye. For reference, a platinum subdermal needle electrode was placed into the forehead of the mouse. Scotopic ERG was performed at six varying flash intensities (-24, -14, -4, 0, and 10 dB) on *Reep6* mutant mice and isogenic control mice at various time intervals (2, 8, and 54 wk postinjection) after subretinal injection treatments. Age-matched *Reep6*^{+/-} untreated mice *Reep6*^{+/-} left eye-injected mice were recorded alongside mutant *Reep6*^{L135P/-} left eye-injected mice at every time point. The LKC UTAS visual diagnostic system and EMWIN software (LKC Technologies) were used to obtain and com-

pile the data. ERG data analysis was performed on GraphPad Prism5 software (GraphPad Software). ERG responses for each flash intensity were averaged from the left-eye (untreated) and right-eye (treated) ERG recordings for each genotype group, and standard *t*-test/one-way ANOVA was performed for statistical analysis as appropriate.

Histology and immunostaining

Individual mice were placed into a small container with isoflurane-infused paper towels and were cervically dislocated after they were anesthetized. Eyes were enucleated and processed in fresh modified Davidson's fixative⁴³ for 18 to 24 h at 4°C. After fixation, eyes were dehydrated in ethanol and embedded in paraffin wax according to standard protocol.^{3,4,44} Serial paraffin sections (7 μ m) were sectioned on a microtome (Leica), and hematoxylin and eosin (H&E) staining was performed. After H&E staining, slides were cleaned, mounted with coverslips, dried at room temperature, and imaged with a light microscope (Apo-Tome; Zeiss). For immunostaining, tissue sections were processed in xylene for 1 h and rehydrated in ethanol gradients. For antigen retrieval, slides were boiled in containers containing 0.01 M citrate buffer in a rice cooker for 30 min, cooled for 30 min on ice, and rinsed in phosphate-buffered saline (PBS) three times. Hybridization was performed using 10% normal goat serum with 0.1% Triton-X100 in PBS for 1 h in a humidifying chamber at room temperature, after incubation with primary antibodies. Antibodies used in this article include REEP6 (kind gift from A. Swaroop, National Eye Institute), M2 FLAG (F3165; Sigma), guanylyl cyclase 1 (Ret GC1 CAT rabbit polyclonal; a kind gift from A. Dizhoor, Salus University), and caspase-12 (ab3612; EMD Millipore). After overnight incubation at 4°C, slides were rinsed in PBS and stained with 4',6-diamidino-2-phenylindole (DAPI; Life Technologies), and Prolong Gold antifade reagent (Life Technologies) was used to mount the coverslips on the slides. An Axio Imager.M2m (Zeiss) was used to obtain immunofluorescence images at $\times 10$, $\times 20$, and $\times 40$ zoom.

RESULTS

Reep6^{L135P/-} compound heterozygous mice exhibit photoreceptor degeneration

Reep6 homozygous null mice exhibit early-onset photoreceptor dysfunction, which is evident starting as early as postnatal day 15 (P15). By P20, photoreceptor degeneration can be observed by histological analysis.³ In comparison, *Reep6*^{L135P/L135P}

homozygous mutant mice exhibit delayed-onset retinal degeneration that is not evident until 2 months or later.⁴ To establish a *Reep6* mouse model that has a proper window of treatability, we generated compound heterozygous mice harboring both a null allele and a missense (L135P) mutant allele, termed *Reep6*^{L135P/-}. Histological analysis of compound heterozygous *Reep6*^{L135P/-} mouse retina revealed defects in retinal morphology compared with the control *Reep6*^{+/-} mouse retina, as expected (Fig. 1). *Reep6*^{L135P/-} mice exhibited mild thinning of the outer nuclear layer (ONL) on P22 (Fig. 1A),

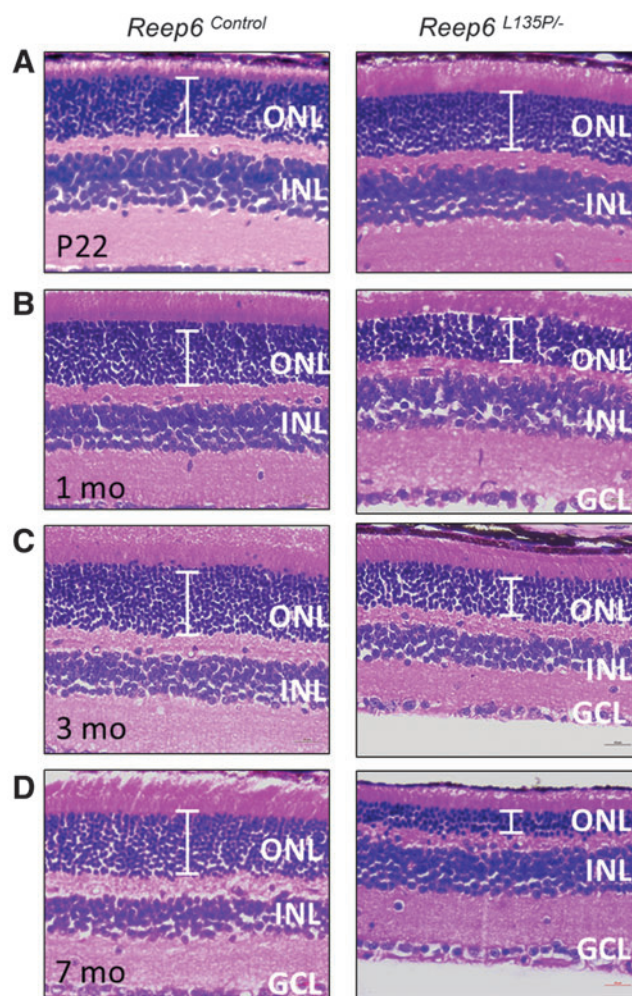


Figure 1. *Reep6*^{L135P/-} compound heterozygous mice exhibit photoreceptor degeneration. Histological analysis of retinal sections from *Reep6*^{L135P/-} and *Reep6*^{+/-} mice was performed on (A) postnatal day 22 (P22) and at (B) 1 month, (C) 3 months, and (D) 7 months of age. *Reep6*^{+/-} retina shows healthy photoreceptor morphology comparable to *Reep6*^{L135P/-} retina on P22, which exhibits mild to no changes in ONL thickness. However, at 1 month, 3 months, and 7 months of age, progressive thinning of the ONL is observed in *Reep6*^{L135P/-} mice compared with the *Reep6*^{+/-} control mice, whereas the INL and GCL remain unaffected. GCL, ganglion cell layer; INL, inner nuclear layer; ONL, outer nuclear layer. Scale bars: 20 μ m. Color images are available online.

which became more severe over time (Fig. 1C–E). By 3 months of age, the retina of *Reep6*^{L135P/−} mice had lost 40% of the photoreceptor cells as indicated by the reduced thickness of the ONL (Fig. 1C). In 7-month-old *Reep6*^{L135P/−} mice, the retina is considerably degenerated with more than 65% of photoreceptor cells lost, and a thin ONL with only a few photoreceptor rows remaining (Fig. 1D). In comparison, the other cell layers in the retina, including the inner nuclear layer and ganglion cell layer (GCL), did not exhibit any obvious defects.

***Reep6* mutant mice exhibit reduced electrophysiological response to light**

Full-field electroretinography (ERG) of dark-adapted *Reep6*^{L135P/−} mice was performed to evaluate the rod photoreceptor-mediated responses at various stages of degeneration. *Reep6*^{L135P/−} mice exhibited a significant reduction in the scotopic ERG responses as early as P22 compared with heterozygous *Reep6*^{+/−} and *Reep6*^{+/L135P} littermate controls (Fig. 2A). The amplitudes of both the a-wave (measuring responses of photoreceptor cells) and b-wave (measuring the cumulative response of rod and bipolar cells) were considerably decreased in *Reep6*^{L135P/−} mice, suggesting that the rod photoreception function is significantly compromised in mice devoid of REEP6. Furthermore, we tested the ERG responses at additional time intervals, including 3 months and 7 months of age, and consistently observed a significant reduction in the a-wave and b-wave responses, whereas the responses were normal in age-matched *Reep6*^{+/L135P} and *Reep6*^{+/−} control mice (Fig. 2B–D).

rAAV-mediated REEP6 transduction in photoreceptor cells

To specifically target REEP6 to the photoreceptors, where it is normally localized in the inner segment of rod cells, we used rAAV8 to package mouse *Reep6.1* complementary DNA (cDNA), the retina-specific isoform of *Reep6*. Expression of the *Reep6.1* construct is under the control of the human rhodopsin kinase (hGRK1) promoter, which has been established to be the most effective combination for attaining rapid and high transgene expression in mouse photoreceptors.⁴⁵ Furthermore, to distinguish the vectored wild-type REEP6.1 protein from the resident REEP6 L135P protein, an N-terminal FLAG tag was included. Because the onset of photoreceptor degeneration in *Reep6*^{L135P/−} mice occurs at or before P22, we performed treatments with rAAV8-*Reep6.1* in mice as early as P20. To determine whether the rAAV8-

Reep6.1 treatment is successful in targeting expression of mouse REEP6 in the photoreceptors, we examined the retina of treated mice ($n=6$) by immunofluorescence staining 2 months posttreatment. In this study, all treatments were performed in the right eye (RE) and compared with the contralateral left eye (LE).

In *Reep6*^{L135P/−} mice, we failed to detect expression of endogenous REEP6 (green) in the LE (Fig. 3A and C). In the treated RE of *Reep6*^{L135P/−} mice, FLAG-tagged transgene expression was robustly detected by positive FLAG staining (red) in the photoreceptors (Fig. 3B). At higher magnification, the FLAG signal was detected specifically in the inner segment of photoreceptors (Fig. 3D) of treated *Reep6*^{L135P/−} retinas, where the wild-type REEP6 protein is normally localized (Fig. 3E). Further, we performed coimmunostaining of *Reep6*^{L135P/−} LE and RE retinal sections with an anti-REEP6 antibody. REEP6 immunolabeling was detected in the inner segment of the photoreceptors in *Reep6*^{L135P/−} RE treated retinal sections, where it colocalized with FLAG-positive staining (Fig. 3B and D). Furthermore, both FLAG and REEP6 immunoreactivity were strongest at the site of injection (indicated by asterisks; Fig. 3B), and the expression extended throughout most of the retina, covering more than 70% of the dorsal and ventral regions. Some regions of the tissue exhibited weaker immunoreactivity due to the inconsistent nature of subretinal injections. Consistent with the expression pattern of REEP6, the areas that were targeted exhibited preservation of overall retinal morphology compared with areas that remained untreated, where marked thinning of the retina was observed on gross examination. On the basis of the data, it is evident that the rAAV8-*Reep6.1* vector results in stable and efficient expression of REEP6 in rod photoreceptors of *Reep6*^{L135P/−} mice after treatment by subretinal injections.

Preservation of photoreceptor integrity and function in rAAV8-*Reep6.1*-treated *Reep6* mutant mice

As previously stated, the retina of *Reep6*^{L135P/−} mice exhibits mild thinning of the ONL starting on P22, which progressively increases in severity. To determine whether the rAAV8-*Reep6.1* treatment was successful in restoring retinal morphology in *Reep6* mutant mice, we performed histological analysis of both the LE and RE of *Reep6*^{L135P/−} mice ($n=6$) 2 months postinjection (referred to as 11 wk old). H&E staining of the untreated LE in 11-week-old mice shows reduction in overall retinal thickness and marked thinning of the ONL (Fig. 4A

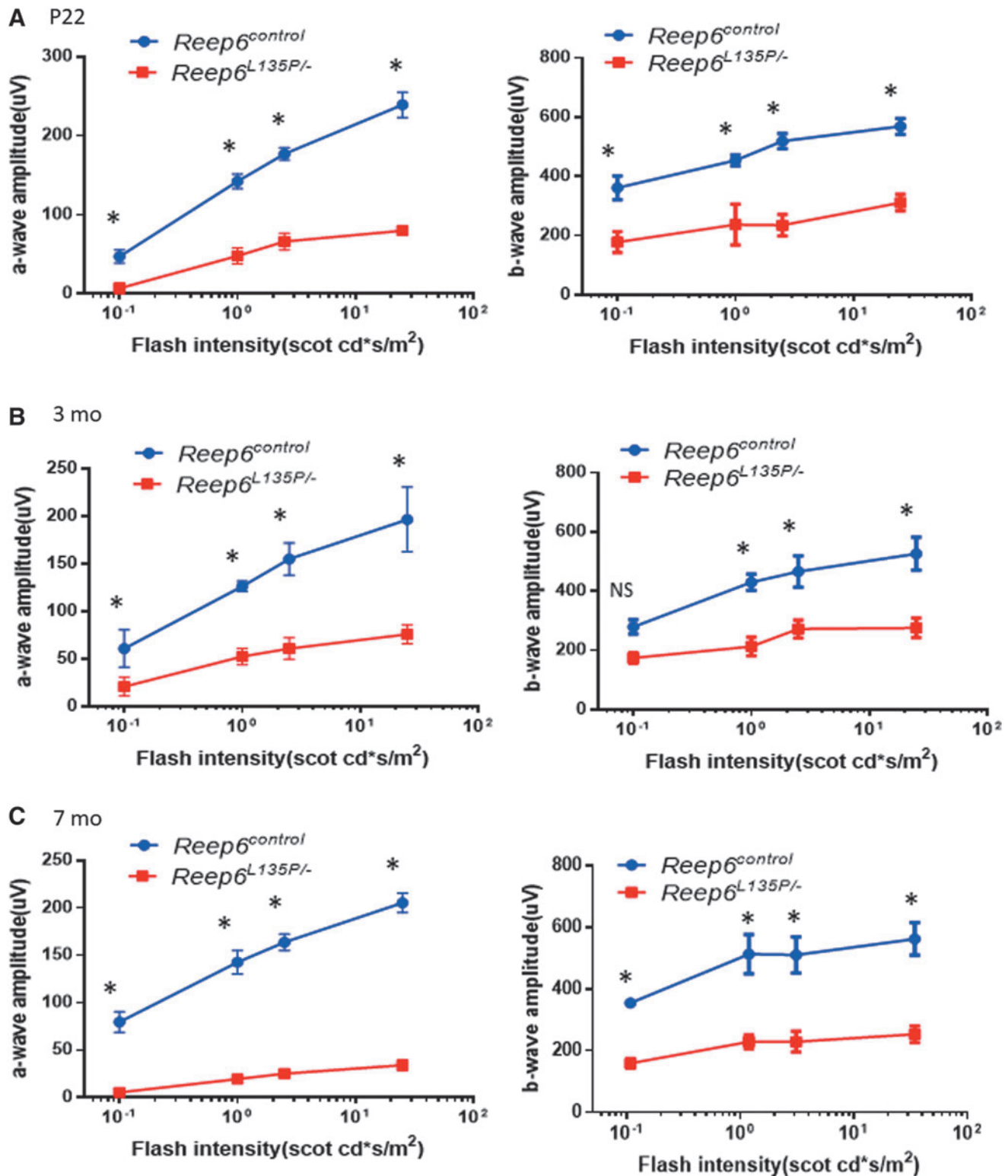


Figure 2. *Reep6*^{L135P/-} mutant mice exhibit defects in response to light. Quantitative evaluation of scotopic a-wave and b-wave responses for dark-adapted mice on (A) postnatal day 22 (P22) and at (B) 3 months and (C) 7 months of age. *Reep6*^{control} (blue line) and *Reep6*^{L135P/-} mice (red line). *Reep6*^{L135P/-} mice exhibited decreased electroretinogram responses at all time points. NS, not significant. *Significance ($p < 0.05$) determined by Student *t*-test. Error bars denote the SEM. Color images are available online.

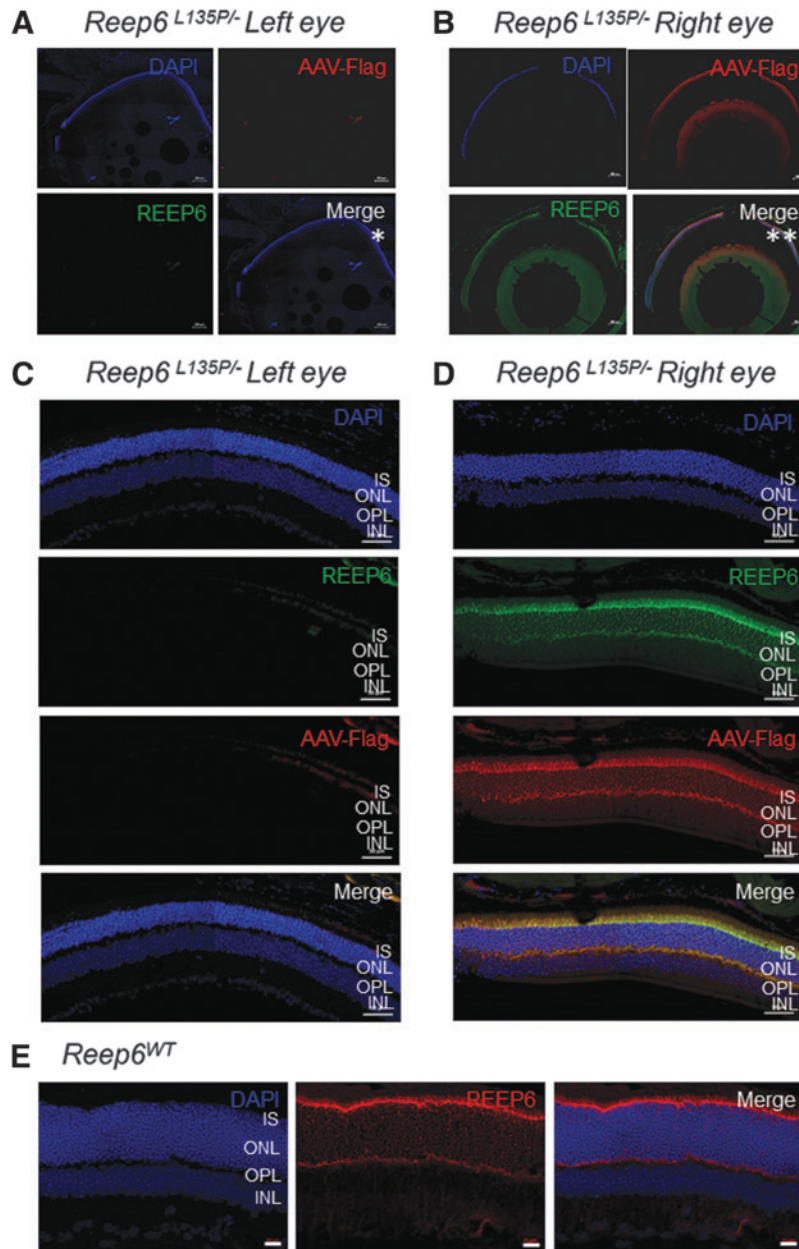


Figure 3. Flag-REEP6.1 and endogenous REEP6 expression and localization in the photoreceptors of rAAV8-*Reep6.1*-treated and -untreated *Reep6*^{L135P/-} mice. Immunofluorescence staining of representative contralateral (A) untreated left eye (LE) of *Reep6*^{L135P/-} mouse retina and (B) treated right eye (RE) of *Reep6*^{L135P/-} mouse retina at 2 months postinjection performed on postnatal day 20. FLAG tag signal (red) was detectable only in the treated right eye of *Reep6*^{L135P/-} mice; REEP6 was undetectable in the untreated LE of *Reep6*^{L135P/-} mice, whereas in the RE, robust staining was detected throughout the retina. The site of injection is indicated by asterisks (**) in (B). DAPI staining was performed to stain for cell nuclei. (C) High-magnification image of *Reep6*^{L135P/-} mouse LE shows no detectable expression of FLAG or REEP6, whereas DAPI staining (blue) shows the presence of photoreceptor nuclei in the ONL. (D and E) In the RE (D), specific targeting of FLAG (red) and REEP6 (green) was detected in the inner segment primarily, and in the perinuclear regions of the ONL and OPL, comparable to endogenous expression of REEP6 in *Reep6* wild-type (WT) retina (E). INL, inner nuclear layer; IS, inner segment; ONL, outer nuclear layer; OPL, outer plexiform layer. Scale bars: (A and B) 200 μm ; (C and D) 50 μm . Images were obtained at $\times 40$ original magnification on a Zeiss ApoTome, and tiling was performed to cover the entire retinal tissue sections (A and B). *Region of magnification in (A) used for imaging in (C); **region of magnification in (B) used for imaging in (D). Color images are available online.

and B), in comparison with treated *Reep6*^{L135P/-} REs and *Reep6* wild-type control mice (Fig. 4C and D). On treatment with rAAV8-*Reep6.1*, *Reep6*^{L135P/-} mouse REs showed drastic improvements in overall retinal morphology as evident by

preservation of photoreceptor cell nuclei in the ONL and increased ONL thickness (Fig. 4C and D) in regions where REEP6 is robustly expressed (Fig. 3B and D). Consequently, in areas of the retina distant from the site of injection and that lack

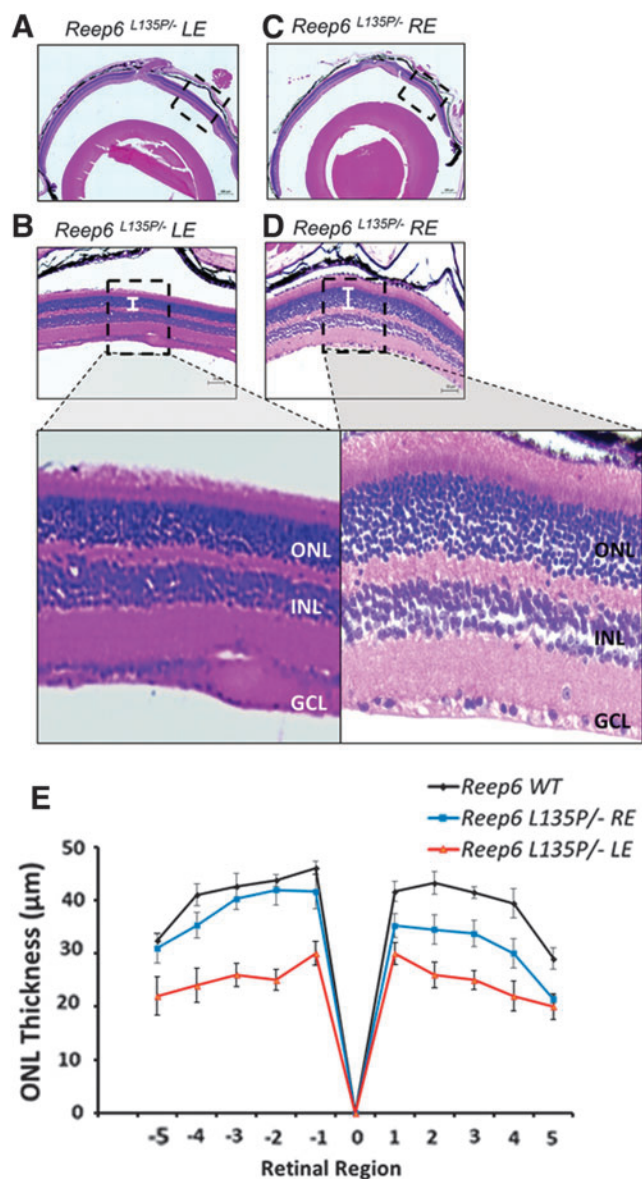


Figure 4. Preservation of photoreceptor morphology in *Reep6*^{L135P/-} mice 2 months after treatment. Shown are hematoxylin and eosin staining of paraffin-embedded retinal sections from (A and B) untreated left eye (LE) and (C and D) treated right (RE) 2 months after injection, performed to assess morphological changes in *Reep6*^{L135P/-} mice. Severe thinning of the ONL was observed in the LE (A); magnified image of the LE affected region is shown in (B). Improvements in the ONL thickness were observed in the RE (C); magnified image of the RE treated region is shown in (D). (E) Retinal morphometry was performed to compare ONL thickness among *Reep6*^{L135P/-} control untreated mouse retinas, *Reep6*^{L135P/-} untreated LE, and *Reep6*^{L135P/-} treated RE, using averaged values obtained from $n=6$ mice per genotype. The butterfly plot includes ONL thickness measured from 10 equally spaced positions along the vertical median of the retina for six retinas of the same genotype. Each point represents the mean \pm SEM obtained for each group. Position 0 corresponds to the optic nerve head. GCL, ganglion cell layer; INL, inner nuclear layer; ONL, outer nuclear layer; WT, wild type. Error bars denote the SEM. Color images are available online.

REEP6 expression, the retinal morphology was less intact in the RE, but improved nonetheless compared with the untreated LE. Quantitative morphometric analysis of *Reep6* wild-type, *Reep6*^{L135P/-} LE, and *Reep6*^{L135P/-} RE shows the ONL thickness averaged from six retinas per group; evidently, there is an improvement in the morphology of the photoreceptors in the treated group.

To assess whether morphological preservation of photoreceptors in *Reep6*^{L135P/-} mice posttreatment is concordant with functional rescue of electrophysiological response to light, we examined the ERGs of dark-adapted *Reep6*^{L135P/-} mice by testing both the LE and RE independently. At 11 weeks of age (2 mo posttreatment on P20), *Reep6*^{L135P/-} mice exhibited an attenuated scotopic ERG response in the contralateral untreated LE, where both the a-wave amplitude and the b-wave amplitude were significantly decreased (indicated by an asterisk) (Fig. 5A and B, red line) compared with healthy *Reep6* wild-type mice (black line). In comparison, the treated RE of *Reep6*^{L135P/-} mutant mice had improvements in the dark-adapted scotopic response at various flash intensities. There was a statistically significant improvement in the a-wave response (indicated by a hashtag symbol); the b-wave (combined rod photoreceptor and inner retinal neurons response) response was also improved, although not significantly. Furthermore, there was no significant difference between the treated RE and the wild-type scotopic b-wave responses (Fig. 5A and B, blue line), demonstrating functional retention of rod photoreceptors resulting from expression of the *Reep6.1* transgene

rAAV8-*Reep6.1*-mediated gene therapy alleviates ER stress response resulting from REEP6 deficiency and restores guanylyl cyclase 1 localization

Previously, we reported that loss of REEP6 causes induction of the ER stress response pathway and activation of signature ER stress markers in *Reep6* homozygous knockout mice on P20, before any major phenotypic defects can be observed. In *Reep6*^{L135P/-} mice, we observed activation of caspase-12, a marker of ER stress-induced apoptosis, in the untreated LE at 11 weeks of age (Fig. 6B). Close examination of caspase-12-positive staining shows a punctate pattern in the ONL (shown by arrows) at higher magnification (Fig. 6B), suggesting activation of the ER stress/unfolded protein response pathway. In 2-month posttreatment RE of *Reep6*^{L135P/-} mice (Fig. 6A), we failed to detect strong positive signals for

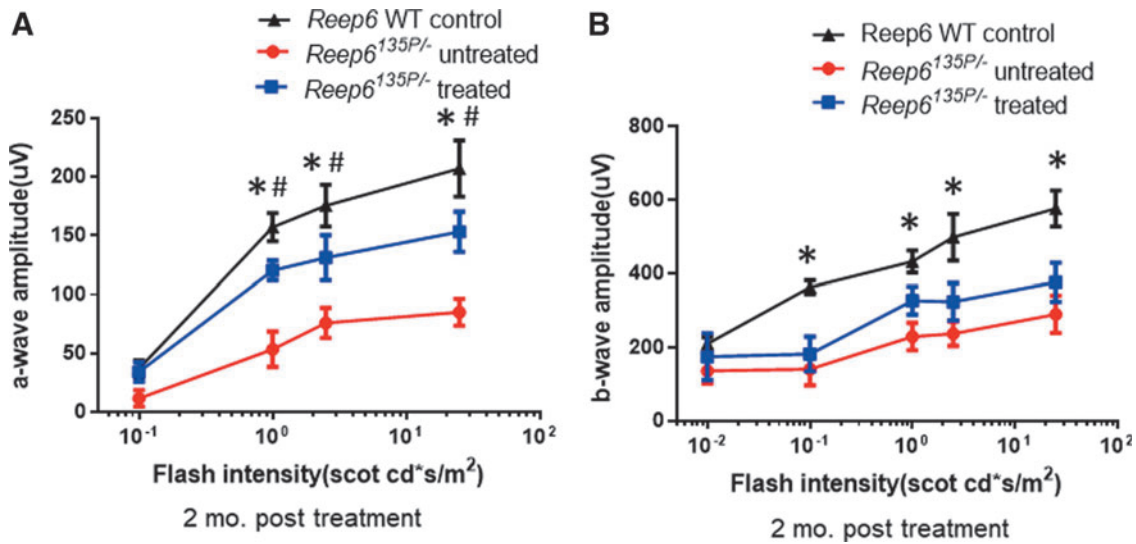


Figure 5. Functional assessment of scotopic response in rAAV8-*Reep6.1*-treated mice based on electroretinography (ERG). Before ERG, fundus examination was performed to check for any damage that was persistent after subretinal injections of all mice. Mice that incurred retinal damage were excluded from ERG analysis. ERG was performed in dark-adapted *Reep6*^{L135P/-} mouse left eye (LE) and right eye (RE) 2 months after treatment at various flash intensities (x axis). **(A)** Averaged a-wave amplitudes (y axis) of *Reep6*^{L135P/-} RE (blue line) and LE (red line) are shown, representing treated versus untreated ERG responses. In addition, a-wave amplitudes of untreated LEs of *Reep6* wild-type (WT) age-matched mice (black line) are included for comparison. **(B)** Averaged b-wave (y axis) amplitudes of *Reep6*^{L135P/-} RE (blue line), LE (red line), and WT (black line) eyes at variable flash intensities (x axis). $n=6$ mice were used to assay LE and RE ERGs. $n=4$ wild-type mice were used as technical controls. Statistical analysis performed by one-way ANOVA. Statistical analysis is denoted with the following symbols: wild-type versus untreated ($*p<0.05$), and untreated versus treated ($#p<0.05$). Error bars denote the SEM. Color images are available online.

caspase-12, suggesting that rAAV8-*Reep6.1* gene therapy can alleviate ER stress response in *Reep6* mutant mice and prolong photoreceptor cell survival.

Furthermore, we have previously shown that guanylyl cyclase 1 (GC1) and GC2 expression in *Reep6* KO mice is undetectable by immunofluorescence microscopy.³ To determine whether REEP6 expression can rescue endogenous expression of GC1 to the photoreceptor outer segment (OS), we performed immunostaining on retinal sections from *Reep6*^{L135P/-} mice 2 months post-treatment. GC1-positive staining was detected in the OS of *Reep6*^{L135P/-} right eye, and the expression was consistent throughout the retina and coincided with FLAG expression in the posttreated eyes. GC1 localization to the OS was comparable to wild-type GC1 localization. In contrast, GC1 expression was not detected in the untreated eyes of *Reep6*^{L135P/-} mice, consistent with the findings observed in *Reep6* KO mice, as expected.

Long-term rescue efficiency of rAAV8-*Reep6.1*-mediated gene therapy in *Reep6* mutant mice

Retinal sections of both LE and RE from *Reep6*^{L135P/-} mice ($n=4$) treated only once on P20 were examined to determine the long-term potential of rAAV8-*Reep6.1* gene therapy treatment. At the late-stage 1-year time point, the ONL of the

untreated LE retina was reduced to only two or three layers of nuclei, consistent with the progressive degeneration observed between P22 and 7 months of age (Fig. 7A). In contrast, rAAV8-*Reep6.1*-treated retina exhibited substantial ONL thickness in the RE of *Reep6*^{L135P/-} mice (Fig. 7B), indicating significant retention of the photoreceptor integrity after prolonged treatment. In addition to restoration of retinal morphology, *Reep6*^{L135P/-} mouse RE also retained a functional photoreponse as measured by ERGs in dark-adapted mice (Fig. 7C and D). Whereas *Reep6*^{L135P/-} mouse LE had a severely diminished a-wave amplitude, the *Reep6*^{L135P/-} mouse RE had a significantly increased a-wave amplitude (Fig. 7A). Similarly, the treated RE of *Reep6*^{L135P/-} mice had an elevated b-wave response (Fig. 7B). On the basis of the comparative ERG analysis, it is evident that rod photoreceptor response is significantly preserved in *Reep6* mutant mice, even up to 1 year posttreatment.

DISCUSSION

Ultimately, the goal of identifying the genetic causes underlying RP is to develop therapeutic treatments for patients who have retinal degeneration; however, to date, there are no gene therapy treatments for patients with autosomal recessive

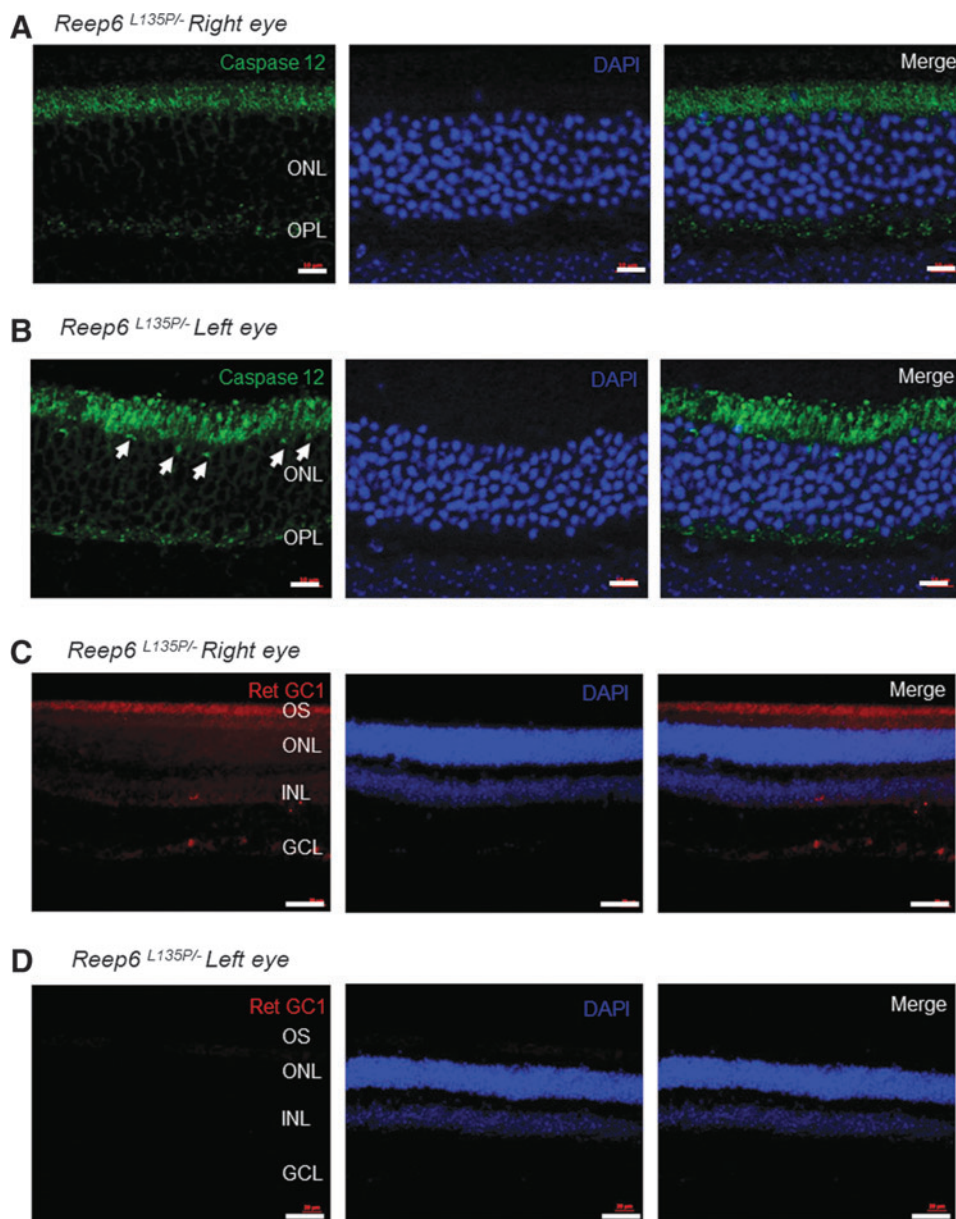


Figure 6. rAAV8-*Reep6.1*-mediated gene therapy alleviates endoplasmic reticulum (ER) stress response and restores guanylyl cyclase 1 (GC1) expression. (**A** and **B**) ER stress was evaluated by immunostaining with ER stress marker caspase-12 in retinal sections from 2-month posttreated right eye (RE) (**A**) and left eye (LE) (**B**) of *Reep6*^{L135P/-} mice. Caspase-12 (green)-positive staining (*arrows*) was observed in the ONL of *Reep6*^{L135P/-} LE retina but was absent from the RE posttreatment. (**C** and **D**) Retinal guanylyl cyclase 1 (Ret GC1) immunostaining in retinal sections from 2-month posttreated RE (**C**) and LE (**D**) of *Reep6*^{L135P/-} mice. Ret GC1 (*red*)-positive staining was detected in the OS of *Reep6*^{L135P/-} RE, whereas it was absent from the LE. Nuclei are counterstained with DAPI (*blue*). GCL, ganglion cell layer; INL, inner plexiform layer; ONL, outer nuclear layer; OPL, outer plexiform layer; OS, outer segment. Scale bars: 10 μ m. Color images are available online.

RP. With emerging findings of success in clinical trials for gene therapy-based approaches to prevent and/or restore loss of photoreceptor cells in the retina, there is evidence for translation of these treatment strategies in humans.^{25–38} Thus, this study set out to develop rAAV-based gene therapy for *REEP6*-associated RP to assess its therapeutic efficacy in *Reep6* mutant mice as a preclinical model of retinal degeneration. Here, we have

shown that compound heterozygous *Reep6*^{L135P/-} mice exhibit progressive retinal degeneration, similar to the clinical observations of an individual who harbored these variants, and that rAAV8-*Reep6.1* regulated by the hGRK1 promoter can effectively drive mouse REEP6 expression in the rod photoreceptors, which results in restoration of retinal morphology and photoreceptor function. This effect of gene replacement therapy can persist

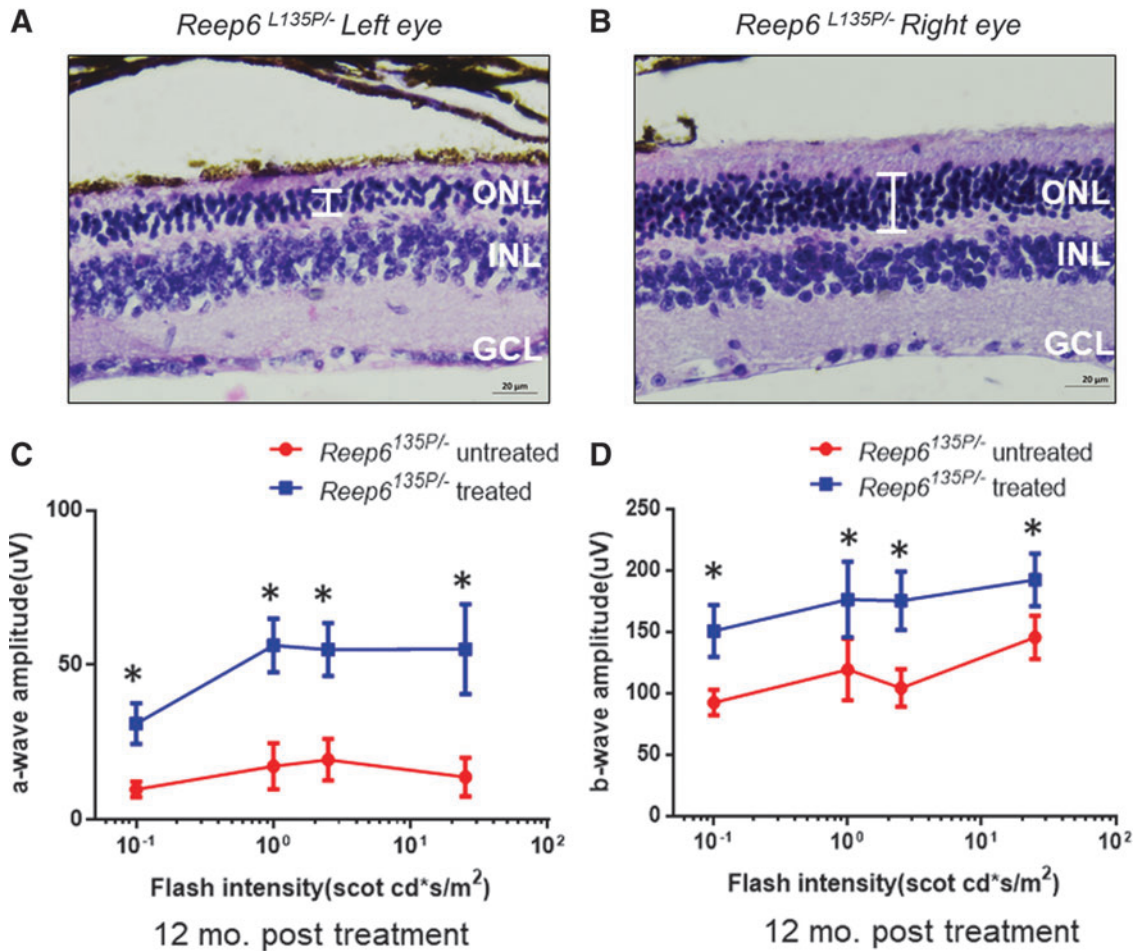


Figure 7. Long-term rescue efficiency of rAAV8-*Reep6.1*-mediated gene therapy in *Reep6* mutant mice. **(A and B)** Long-term improvement of photoreceptor degeneration was observed in postnatal day 20 (P20)-treated mice at 1 year posttreatment. A representative untreated left eye (LE) of *Reep6*^{L135P/-} mice shows robust loss of ONL and overall thinning of the retina **(A)**. The RE treated retina shows a thicker ONL compared with the contralateral untreated retina, with about 70% of photoreceptor survival compared with healthy wild-type retina at 1 year of age **(B)**. **(C)** ERG analysis shows significant improvement in light response of dark-adapted animals 1 year posttreatment in the RE (blue line) compared with the LE (red line), which exhibits severely diminished responses at various flash intensities. **(D)** b-Wave amplitudes of the *Reep6*^{L135P/-} RE showed improvement in the cumulative response of rod/bipolar cells (blue line) compared with the untreated LE (red line). Statistical analysis performed by one-tailed paired *t*-test. *n*=4 mice were used to perform histological analysis and ERGs. *Significant at *p*<0.05 determined by Student *t*-test. Error bars denote the SEM. Color images are available online.

up to 1 year postinjection, demonstrating its long-term therapeutic potential in treating retinal degeneration. Importantly, transgene expression of *Reep6.1*, the retina-specific isoform of *Reep6*, induced proper GC1 expression and localization to the OS, resulting in alleviation of ER stress and restoration of visual function and photoreceptor survival.

We have established and characterized two animal models of *REEP6*-associated retinal degeneration.^{3,4} *Reep6*^{L135P/L135P} mice exhibit adult-onset photoreceptor degeneration that is evident at about 4 months of age, whereas *Reep6* germline-null mutant mice exhibit a much more severe, rapid onset of retinal dysfunction, which precedes retinal degeneration, as early as P15. In the

REEP6-associated RP cohort, two mutations, a missense mutation (c.404T>C [p.Leu135Pro]) and a single-nucleotide deletion also in exon 4 (c.448del [p.Ala150Pfs*2]), were identified in an individual with RP. To recapitulate the genotype of this individual, which we deemed would be an interesting model to assess the efficacy of gene therapy, we generated compound heterozygous *Reep6*^{L135P/-} mice. *Reep6*^{L135P/-} mice exhibit photoreceptor dysfunction that is evident by P22, although the morphological defects become evident at about 1 month of age. Furthermore, although *Reep6*^{L135P/-} mice display the presence of at least three photoreceptor layers by 1 year of age, *Reep6*^{-/-} mice have merely one photoreceptor layer remaining in the late stages of disease progression. Thus, the se-

verity of degeneration observed in *Reep6*^{L135P/-} mice is modestly mild compared with the pathogenesis observed in *Reep6* KO mice, making it an ideal candidate for gene therapy clinical trials as it provides an optimal window of treatment to evaluate its therapeutic potential.

The retina-specific isoform of *Reep6*, referred to as *Reep6.1*, was identified by gene expression profiling of *Nrl* KO mice,¹⁸ and is expressed specifically in rod photoreceptors. Compared with the canonical transcript, termed *REEP6.2*, we have shown that *REEP6.1* is the predominant isoform in developing human photoreceptors and, indeed, *REEP6.1* expression appears to be limited to rod photoreceptors in human 3D optic cups. We performed further analysis to look at the transcripts of both *REEP6* isoforms in human tissues and confirmed that *REEP6.1* is the predominant isoform expressed in the human retina. Furthermore, we have reported a biallelic single-nucleotide duplication within intron 4 of the *REEP6.2* isoform that causes premature termination of the *REEP6.1* isoform (c.557dupC [p.Val187Glyfs*13]) in an affected individual, whereas *REEP6.2* remains unperturbed.⁴ Collectively, these findings suggest that *REEP6.1* is a novel transcript within rod photoreceptors, where it likely plays essential roles in retinal function/homeostasis, disruption of which results in the observed retinal dystrophy phenotypes in mice and patients. Thus, in this study, we chose to deliver species-specific *Reep6.1* cDNA to photoreceptors packaged in the rAAV8 vector to evaluate the therapeutic potential of gene therapy and to gain further insights into the role of *REEP6.1* specifically in rod photoreceptors.

On treatment of *Reep6*^{L135P/-} mice RE with rAAV8-*Reep6.1*, we observed rapid and robust expression of both FLAG and *REEP6* in the retina, where they colocalized to the inner segment of the photoreceptors. These data provided confirmation that the hGRK1 promoter was successful in restricting expression of *REEP6* to photoreceptors, and no off-target expression resulted in the retina because of overexpression of the rAAV8-*Reep6.1* viral vector. Furthermore, treatment of the RE of *Reep6*^{L135P/-} mice enhanced photoreceptor cell survival and preserved the scotopic response to light under dark-adapted conditions. On the basis of analysis of the a-wave (photoreceptor response) in the RE versus the LE of *Reep6* mutant mice, there was a significant improvement in the ERGs. However, the improvement in the b-wave (combined photoreceptor and inner retinal neurons response) was not as strong as that of the a-wave, which may reflect an underlying secondary defect

in the second-order neurons in the inner retina. In this study, we did not measure the isolated response of bipolar cells, which could provide further insights regarding the ERG b-wave data obtained.

As expected, the improvements in retention of photoreceptor integrity and function led to an alleviated ER stress response in the RE, whereas the untreated LE had strong caspase-12-positive staining present throughout the retina. It is known that induction of the ER stress pathway and the unfolded protein response can lead to ER stress-induced apoptosis, which results in photoreceptor cell death.⁴⁶⁻⁵¹ Here, we have shown that treatment with rAAV8-*Reep6.1* is sufficient in rescuing this fate, allowing the photoreceptors to survive and function properly for an extended period of time posttreatment. Indeed, several already established mouse models of retinal degeneration exhibit ER stress, and it would be of interest to determine whether therapeutic approaches such as targeted gene therapy for these other mice can also have a similar effect in alleviating the cell stress response.

On the basis of the positive results obtained from gene therapy trials in *Reep6* mutant mice, we also wanted to investigate the molecular mechanisms involved in restoration of visual function and photoreceptor survival. Previously, we have shown that loss of *Reep6* leads to misexpression and/or mistrafficking of select proteins involved in the phototransduction pathway. GC1 function is integral in the synthesis of cyclic GMP (cGMP) in the retina, which regulates the opening/closing of cGMP-gated channels, which in turn leads to depolarization/hyperpolarization of the photoreceptors, respectively.³ In *Reep6* KO mice, we hypothesized that when GC1 function is compromised, depletion of intracellular cGMP leads to failure of opening of the cGMP-gated ion channels, resulting in prolonged hyperpolarization of the rod photoreceptors, eventually leading to overexertion and subsequent cell death. The rescue of GC1 localization to the OS by *Reep6* transgene expression in the photoreceptors validates our previous hypothesis. It also coincides well with the elevated ERG response posttreatment, indicating that the phototransduction machinery has likely been restored in *Reep6*^{L135P/-} mutant mice.

In addition, we observed preservation of rod photoreceptor ERG responses as well as increased photoreceptor survival in mice up to 1 year posttreatment after just one round of treatment. This strong effect of rAAV8-*Reep6.1* gene therapy can likely be attributed to the high transduction rate of the viral vector in the photoreceptors, as well as

proper localization of FLAG-tagged *Reep6.1*. Indeed, *Reep6.1*-FLAG-tagged transgene expression sufficiently replenished endogenous REEP6 expression and localization in the retina, illustrating that proper targeting of rAAV-based vectors in the appropriate regions of interest has a significant impact on the overall therapeutic potential. In future, it would be interesting to investigate the effects of restoring the canonical isoform, *Reep6.2*, using similar approaches utilized in the current study to determine whether it has the potential to rescue photoreceptor degeneration in *Reep6* mutant mice.

In conclusion, this work highlights the success of the first clinical rAAV8-*Reep6.1*-based gene therapy in *Reep6* mutant mouse models of retinal degeneration. In particular, we show that 2 months and up to 1 year posttreatment, *Reep6* mutant mice showed improvements in the photoresponse as well as preservation of photoreceptor cells, demonstrating that the treatment is effective even after a prolonged period of time. Findings from this study show that gene replacement therapy in the retina with rAAV8-*Reep6.1* can improve photoreceptor function in *Reep6* mutant mice, extend survival of photorecep-

tors *in vivo*, and can be potentially used as a therapeutic target for treatment of patients with RP.

ACKNOWLEDGMENTS

The authors thank the Genetically Engineered Mouse Core, which is partially supported by National Institutes of Health (NIH) grant P30CA125123 at the Baylor College of Medicine for generating *Reep6* mouse models using CRISPR-gene editing. The authors also thank the Gene Vector Core at the Baylor College of Medicine. This project was funded by the Foundation Fighting Blindness (BR-GE-0613-0618-BCM), the National Eye Institute (R01EY022356, R01EY020540) to R.C., and by 5T32EY007102-23 awarded to S.A. (PI: Dr. Graeme Mardon).

AUTHOR DISCLOSURE

There is no conflict of interest and/or competing financial interests to be declared by the authors that contributed to this study.

SUPPLEMENTARY MATERIAL

Supplementary Figure S1

REFERENCES

- Daiger SP, Bowne SJ, Sullivan LS. Perspective on genes and mutations causing retinitis pigmentosa. *Arch Ophthalmol* 2007;125:151–158.
- Fahim AT, Daiger SP, Weleber RG. GeneReviews: nonsyndromic retinitis pigmentosa overview. In: R.A. Pagon MP, Adam HH, Ardinger SE, et al, eds. Seattle, WA: University of Washington; 1993 [last update: January 19, 2017]. Available from: <https://www.ncbi.nlm.nih.gov/books/NBK1417/>
- Agrawal SA, Burgoyne T, Eblimit A, et al. REEP6 deficiency leads to retinal degeneration through disruption of ER homeostasis and protein trafficking. *Hum Mol Genet* 2017;26:2667–2677.
- Arno G, Agrawal SA, Eblimit A, et al. Mutations in REEP6 cause autosomal-recessive retinitis pigmentosa. *Am J Hum Genet* 2016;99:1305–1315.
- Hartong DT, Berson EL, Dryja TP. Retinitis pigmentosa. *Lancet* 2006;368:1795–1809.
- Daiger SP, Rossiter B, Greenberg J, et al. Data services and software for identifying genes and mutations causing retinal degeneration. *Invest Ophthalmol Vis Sci* 1998;39:S295.
- Dias MF, Joo K, Kemp JA, et al. Molecular genetics and emerging therapies for retinitis pigmentosa: basic research and clinical perspectives. *Prog Retin Eye Res* 2018;63:107–131.
- Aad G, Abbott B, Abdallah J, et al; ATLAS Collaboration; CMS Collaboration. Combined measurement of the Higgs boson mass in *pp* collisions at $\sqrt{s}=7$ and 8 TeV with the ATLAS and CMS experiments. *Phys Rev Lett* 2015;114:191803.
- Veleri S, Nellisery J, Mishra B, et al. REEP6 mediates trafficking of a subset of clathrin-coated vesicles and is critical for rod photoreceptor function and survival. *Hum Mol Genet* 2017;26:2218–2230.
- Mejcasec C, Mohand-Said S, El Shamieh S, et al. A novel nonsense variant in REEP6 is involved in a sporadic rod-cone dystrophy case. *Clin Genet* 2018;93:707–711.
- Voeltz GK, Prinz WA, Shibata Y, et al. A class of membrane proteins shaping the tubular endoplasmic reticulum. *Cell* 2006;124:573–586.
- Shibata Y, Shemesh T, Prinz WA, et al. Mechanisms determining the morphology of the peripheral ER. *Cell* 2010;143:774–788.
- Hu J, Shibata Y, Voss C, et al. Membrane proteins of the endoplasmic reticulum induce high-curvature tubules. *Science* 2008;319:1247–1250.
- Mainland J, Matsunami H. RAMP like proteins: RTP and REEP family of proteins. *Adv Exp Med Biol* 2012;744:75–86.
- Bjork S, Hurt CM, Ho VK, et al. REEPs are membrane shaping adapter proteins that modulate specific G protein-coupled receptor trafficking by affecting ER cargo capacity. *PLoS One* 2013;8:e76366.
- Park CR, You DJ, Park S, et al. The accessory proteins REEP5 and REEP6 refine CXCR1-mediated cellular responses and lung cancer progression. *Sci Rep* 2016;6:39041.
- Sato H, Tomita H, Nakazawa T, et al. Deleted in polyposis 1-like 1 gene (*Dp1/1*): a novel gene richly expressed in retinal ganglion cells. *Invest Ophthalmol Vis Sci* 2005;46:791–796.
- Hao H, Veleri S, Sun B, et al. Regulation of a novel isoform of receptor expression enhancing protein REEP6 in rod photoreceptors by bZIP transcription factor NRL. *Hum Mol Genet* 2014;23:4260–4271.
- Azadi S, Molday LL, Molday RS. RD3, the protein associated with Leber congenital amaurosis type 12, is required for guanylate cyclase trafficking in photoreceptor cells. *Proc Natl Acad Sci U S A* 2010;107:21158–21163.
- Molday LL, Jefferies T, Molday RS. Insights into the role of RD3 in guanylate cyclase trafficking, photoreceptor degeneration, and Leber congenital amaurosis. *Front Mol Neurosci* 2014;7:44.
- Wright ZC, Singh RK, Alpino R, et al. ARL3 regulates trafficking of prenylated phototransduction proteins to the rod outer segment. *Hum Mol Genet* 2016;25:2031–2044.
- Schwarz N, Lane A, Jovanovic K, et al. Arl3 and RP2 regulate the trafficking of ciliary tip kinesins. *Hum Mol Genet* 2017;26:3451.

23. Hanke-Gogokhia C, Wu Z, Gerstner CD, et al. Arf-like Protein 3 (ARL3) regulates protein trafficking and ciliogenesis in mouse photoreceptors. *J Biol Chem* 2016;291:7142–7155.
24. Eblimit A, Nguyen TM, Chen Y, et al. *Spata7* is a retinal ciliopathy gene critical for correct RRGrip1 localization and protein trafficking in the retina. *Hum Mol Genet* 2015;24:1584–1601.
25. Schön C, Sothilingam V, Mühlfriedel R, et al; RD-Cure Consortium. Gene therapy successfully delays degeneration in a mouse model of PDE6A-linked retinitis pigmentosa (RP 43). *Hum Gene Ther* 2017;28:1180–1188.
26. Occelli LM, Schon C, Seeliger MW, et al; RD-Cure Consortium. Gene supplementation rescues rod function and preserves photoreceptor and retinal morphology in dogs, leading the way towards treating human PDE6A-retinitis pigmentosa. *Hum Gene Ther* 2017;28:1189–1201.
27. Mowat FM, Occelli LM, Bartoe JT, et al. Gene therapy in a large animal model of PDE6A-retinitis pigmentosa. *Front Neurosci* 2017;11:342.
28. Molday LL, Djajadi H, Yan P, et al. RD3 gene delivery restores guanylate cyclase localization and rescues photoreceptors in the Rd3 mouse model of Leber congenital amaurosis 12. *Hum Mol Genet* 2013;22:3894–3905.
29. Mihelec M, Pearson RA, Robbie SJ, et al. Long-term preservation of cones and improvement in visual function following gene therapy in a mouse model of Leber congenital amaurosis caused by guanylate cyclase-1 deficiency. *Hum Gene Ther* 2011;22:1179–1190.
30. Koch S, Sothilingam V, Garcia Garrido M, et al. Gene therapy restores vision and delays degeneration in the *CNGB1*^{-/-} mouse model of retinitis pigmentosa. *Hum Mol Genet* 2012;21:4486–4496.
31. Boye SL, Conlon T, Erger K, et al. Long-term preservation of cone photoreceptors and restoration of cone function by gene therapy in the guanylate cyclase-1 knockout (GC1KO) mouse. *Invest Ophthalmol Vis Sci* 2011;52:7098–7108.
32. Boye SE, Boye SL, Pang J, et al. Functional and behavioral restoration of vision by gene therapy in the guanylate cyclase-1 (GC1) knockout mouse. *PLoS One* 2010;5:e11306.
33. Jacobson SG, Boye SL, Aleman TS, et al. Safety in nonhuman primates of ocular AAV2-RPE65, a candidate treatment for blindness in Leber congenital amaurosis. *Hum Gene Ther* 2006;17:845–858.
34. Jacobson SG, Acland GM, Aguirre GD, et al. Safety of recombinant adeno-associated virus type 2-RPE65 vector delivered by ocular subretinal injection. *Mol Ther* 2006;13:1074–1084.
35. Choi VW, Bigelow CE, McGee TL, et al. AAV-mediated RLB1 gene therapy improves the rate of dark adaptation in Rlb1 knockout mice. *Mol Ther Methods Clin Dev* 2015;2:15022.
36. Zhong H, Eblimit A, Moayed Y, et al. AAV8(Y733F)-mediated gene therapy in a *Spata7* knockout mouse model of Leber congenital amaurosis and retinitis pigmentosa. *Gene Ther* 2015;22:619–627.
37. Petersen-Jones SM, Occelli LM, Winkler PA, et al. Patients and animal models of *CNGβ1*-deficient retinitis pigmentosa support gene augmentation approach. *J Clin Invest* 2018;128:190–206.
38. Zaneveld J, Wang F, Wang X, et al. Dawn of ocular gene therapy: implications for molecular diagnosis in retinal disease. *Sci China Life Sci* 2013;56:125–133.
39. Weleber RG, Pennesi ME, Wilson DJ, et al. Results at 2 years after gene therapy for RPE65-deficient Leber congenital amaurosis and severe early-childhood-onset retinal dystrophy. *Ophthalmology* 2016;123:1606–1620.
40. Le Meur G, Lebranchu P, Billaud F, et al. Safety and long-term efficacy of AAV4 gene therapy in patients with RPE65 Leber congenital amaurosis. *Mol Ther* 2018;26:256–268.
41. Georgiadis A, Duran Y, Ribeiro J, et al. Development of an optimized AAV2/5 gene therapy vector for Leber congenital amaurosis owing to defects in RPE65. *Gene Ther* 2016;23:857–862.
42. Bennett J, Wellman J, Marshall KA, et al. Safety and durability of effect of contralateral-eye administration of AAV2 gene therapy in patients with childhood-onset blindness caused by RPE65 mutations: a follow-on phase 1 trial. *Lancet* 2016;388:661–672.
43. Latendresse JR, Warbritton AR, Jonassen H, et al. Fixation of testes and eyes using a modified Davidson's fluid: comparison with Bouin's fluid and conventional Davidson's fluid. *Toxicol Pathol* 2002;30:524–533.
44. Eblimit A, Agrawal SA, Thomas K, et al. Conditional loss of *Spata7* in photoreceptors causes progressive retinal degeneration in mice. *Exp Eye Res* 2018;166:120–130.
45. Kay CN, Ryals RC, Aslanidi GV, et al. Targeting photoreceptors via intravitreal delivery using novel, capsid-mutated AAV vectors. *PLoS One* 2013;8:e62097.
46. Zhang SX, Sanders E, Fliesler SJ, et al. Endoplasmic reticulum stress and the unfolded protein responses in retinal degeneration. *Exp Eye Res* 2014;125:30–40.
47. Yang LP, Wu LM, Guo XJ, et al. Endoplasmic reticulum stress is activated in light-induced retinal degeneration. *J Neurosci Res* 2008;86:910–919.
48. Jing G, Wang JJ, Zhang SX. ER stress and apoptosis: a new mechanism for retinal cell death. *Exp Diabetes Res* 2012;2012:589589.
49. Griciuc A, Aron L, Ueffing M. ER stress in retinal degeneration: a target for rational therapy? *Trends Mol Med* 2011;17:442–451.
50. Chan P, Stolz J, Kohl S, et al. Endoplasmic reticulum stress in human photoreceptor diseases. *Brain Res* 2016;1648:538–541.
51. Athanasiou D, Aguila M, Bevilacqua D, et al. The cell stress machinery and retinal degeneration. *FEBS Lett* 2013;587:2008–2017.

Received for publication April 10, 2018;
accepted after revision August 10, 2018.

Published online: August 10, 2018.